

ІНСТИТУТ
ФІЗИКИ
КОНДЕНСОВАНИХ
СИСТЕМ

ICMP-01-03E

T.M. Bryk, M.Yu. Druchok, M.F. Holovko and Yu.V. Kalyuzhnyi

MOLECULAR DYNAMICS MODELING OF IONIC VALENCE
INFLUENCE ON THE PROPERTIES OF CATIONS IN
AQUEOUS SOLUTIONS

ЛЬВІВ

УДК: 532:537.226:541.135

РАС: 82.70Dd; 61.20.-p; 61.20.Gy; 61.20.Ne; 61.20.Qg; 02.30.Rz

Моделювання впливу валентності катіона на його властивості у водних розчинах методом молекулярної динаміки

Т.М. Брик, М.Ю. Дручок, М.Ф. Головко, Ю.В. Калюжний

Анотація. Методом молекулярної динаміки зроблено спробу дослідження впливу позитивно зарядженого катіона (валентності від +1 до +6) на структурні і динамічні властивості молекул води в його гідратній оболонці. Виконано детальний аналіз радіальних функцій розподілу і автокореляційних функцій швидкостей. Виявлено ефект утворення високостабільного кластера з молекулами води в вершинах октаедра і катіоном в центрі внаслідок сильної електростатичної взаємодії іон-вода. Показано, що збільшення заряду катіона веде до витягування молекул води в гідратній оболонці і навіть до втрати ними протонів. Досліджено формування гідроксонієвих молекул і більш складних структур. Аналіз автокореляційних функцій швидкостей і їх Фур'є-перетворень для катіона і його шести сусідів вказує на появу нових частот в коливному спектрі гідратної оболонці.

Molecular Dynamics Modeling of Ionic Valence Influence on the Properties of Cations in Aqueous Solutions

T.M. Bryk, M.Yu. Druchok, M.F. Holovko and Yu.V. Kalyuzhnyi

Abstract. Using the technique of molecular dynamics we made the attempt to clarify the effects of the presence of highly charged cations on the structure and dynamics of the water molecules in aqueous solution. Special attention is paid to cation first hydration shell. Analysis of radial distribution functions and velocity autocorrelation functions is performed in detail. It is shown that the strong ion-water electrostatic interaction leads to the formation of stable cluster which consists of six oxygens octahedrally arranged around the cation. The increase of cation valency makes the water molecules in hydration shell to stretch and even loose protons. The formation of hydroxonium molecules and more complicated structures is discussed. The correspondent velocity autocorrelation functions are investigated: the appearance of new frequencies in libration spectra of cation and oxygens from hydration shell is observed.

© Інститут фізики конденсованих систем 2001
Institute for Condensed Matter Physics 2001

1. Introduction

The hydration and hydrolysis of metal ions by water molecules are two initial steps of many processes occurring in metal ion aqueous solutions and playing important role in many natural and industrial processes. The hydration of a metal cation M^{Z+} leads to the formation of complex $[M(H_2O)_n]^{Z+}$, where n is a number of water molecules in hydration shell, so-called hydration number. The hydrolysis leads to decay of water molecules in hydration shell and can be considered as a chain of H^+ -eliminating (acid dissociation) reactions converting hydrated cation complexes into new ionic species $[MO_nH_{2n-h}]^{(Z-h)+}$ where h is a number of protons lost by the water molecules from hydration shell, so-called the molar ratio of hydrolysis [1,2]. Usually the process does not stop at this step and, as a result of the condensation reaction, polynuclear ions appear [2,3]. The nature of these ionic hydrolysed-hydrated species is of the fundamental interest in inorganic solutions chemistry and of particular importance in many areas ranging from nuclear technology to environmental chemistry [4].

The prevalent force in both processes is the strong ion-water interaction in which the electrostatic interaction dominates and increases with increasing of an ionic valency and/or decreasing of an ionic size.

The polarizing power of metal cations leads to formation of the hydration shell around an ion. It can also be sufficiently strong to repel a proton H^+ of water from first hydration shell. This leads to a water molecule dissociation. Under this condition the aqueous metal ion acts as an acid or proton donor and the acid strength of such ion is measured by the acidity constant pK_a . Assuming that the bond character between the cation and the oxygen of water molecules is purely electrostatic, the relationship for acidity and stability of aqueous cations can be expressed in terms of the ionic potential (Z/d) as in [1]

$$pK_a = A - 11.0(Z/d) \quad (1)$$

where Z is the formal charge of cation and d is metal-oxide interatomic distance (in \AA), the constant $A=20-22$ in dependence on electronic configuration of ions. Recently in [5] such linear correlation between acidity constant and binding energy of hydrated cations was derived also from electronic density calculations.

Since the pioneering molecular dynamics (MD) simulation of an aqueous electrolyte solution [6] based on the ST2 model for water [7] was carried out the impressive progress has been achieved in a computer modeling of the structure of ionic hydration shell and dynamic properties of water molecules around ions. Usually such investigations are based

on the use of rigid or flexible models for water molecules and the pair additive interaction models with ion-water interaction potentials derived from empirical knowledge and/or ab initio calculations.

The rigid ST2 model for water was very useful for the description of hydration structure of monovalent alkaline cations (Li^+ , Na^+ , K^+ , Rb^+ , Cs^+) [8,9] since the electrostatic influence of electric field of these cations on water molecules in hydration shell is negligible. However for doubly valent alkaline earth cations (Be^{2+} , Mg^{2+} , Ca^{2+} , Sr^{2+} ,) this effect is already important. The central force (CF) model of water [10,11] is more convenient for this aim. This is the flexible model, in the framework of it the water molecules are considered as a mixture of oxygen and hydrogen atoms bearing partial charges keeping the water molecule geometry solely preserved by an appropriate set of oxygen-hydrogen and hydrogen-hydrogen pair potentials. As a result of non-rigidity of CF model it is possible to study the effects of the influence of ions on the intramolecular properties of water in hydration shell. The MD simulations in the group of Heinzinger [8] for alkaline earth cations with the application of BJH [12] version of CF model for water shown that the strong electrostatic interaction between cation and water molecules leads to the increase of intramolecular OH distance for molecules of water in hydration shell comparing with bulk water.

Simultaneously with increasing of the role of electrostatic cation-water interaction (with increasing of ionic valency and/or decreasing of ionic size) the assumption of pairwise additivity of the ion-water interaction becomes much less justified. The important role of three-body ion-water interactions was demonstrated for Be^{2+} [13], the smallest of the divalent cations, and trivalent Al^{3+} [14,15].

These results for Be^{2+} are confirmed by ab initio molecular dynamics based on a gradient-corrected density functional [15]. However in spite of large efforts to describe the ion-water interaction correctly no hydrolysis effects are taken into account directly in the relevant simulations [13-17]. More successful was thermodynamical treatment of hydrolysis effects for trivalent Fe^{3+} [18,19].

The role of the hydrolysis effects strongly increases for cations of four and higher valency, such as Zr^{4+} , Th^{4+} , U^{4+} , Pu^{4+} . Between them the actinide cations can possess different valence states in aqueous solutions. For example U^{4+} and Pu^{4+} oxidize to the hexavalent form U^{6+} and Pu^{6+} followed by the formation of actinyl form UO_2^{2+} and PuO_2^{2+} [20], which are systematic chemical toxicants that determine a chemical influence of depleted uranium [21].

However despite their considerable importance, studies of hydrolysed-

hydrated form of tetra and higher valent cations are scarce. This is explained by the difficulties of ab initio simulations for such real cations due to large number of electrons of these atoms. For this reason the usual computer simulations are practically unable to derive the interaction potentials between ions and water molecules from ab initio calculations with a sufficient degree of reliability [17].

In this connection at the first step of the investigation of the influence of ionic valency on the properties of cations in aqueous solutions it will be useful to separate the effect of electrostatic interaction between cation and water molecules from other contributions connected with an influence of ionic sizes, nonadditivity of ion-water interactions etc. For this aim the simplified model Na^+ -like cation in the system of flexible water molecules [22] will be very convenient. In this model the potential of the ion-water interaction is similar to the interaction potential of Na^+ with water [23] with assumption that ion can possess the different valency Z . The investigation of the cation valency influence on cation hydration shell structure was carried out for this model in the framework of the integral equations technique [22]. An effect of some protons loss by water molecules from hydration shell was discovered which was treated as the hydrolysis of water caused by ions of high valency.

However these results should be revised by computer simulations technique since the quality of approximations used in integral equation description in [22] needs the improvement in case when ionic valency increases. For this aim in this article we consider a molecular dynamics modeling of the influence of ionic valency on the properties of Na^+ -like cations in aqueous solution. It is shown that a strong ion-water electrostatic interaction leads to the formation of highly stable structures constituted by six water molecules octahedrally arranged around the cations. With cation charge increasing the effect of deprotonation of water molecules from first hydration shell is found. The application of molecular dynamics technique gives also the possibility for investigation of dynamic properties of water molecules around the cations.

2. Model

In our investigations we use the simple model introduced in [22] which for monovalent cation case corresponds to the model which was used for a computer modeling of the aqueous solution of $NaCl$ [23]. For the description of water molecules we use the CF1 model [24,25] which is a slightly modified version of CF model. In this model water is a binary

mixture of oxygen and hydrogen atoms with interparticle interactions:

$$\begin{aligned} U_{OO}(r) &= \frac{144.538}{r} + \frac{26758.2C_1}{r^{8.8591}} - 0.25e^{-4(r-3.4)^2} - 0.25e^{-1.5(r-4.5)^2}, \\ U_{HH}(r) &= \frac{36.1345}{r} + \frac{18}{1 + e^{40(r-2.05C_2)}} - 17e^{-7.62177(r-1.45251)^2}, \\ U_{OH}(r) &= -\frac{72.269}{r} + \frac{6.23403}{r^{9.19912}} - \frac{10}{1 + e^{40(r-1.05)}} - \\ &\quad - \frac{4}{1 + e^{5.49305(r-2.2)}} \end{aligned} \quad (2)$$

where $C_1 = 0.9$, $C_2 = 1/1.025$, the distance is given in Å and energy in kcal/mol.

In CF model hydrogen and oxygen ions have the effective charges $q_H = +0.32983e$ and $q_O = -2q_H$ respectively, where e is the elementary electric charge. Bopp [25] turned our attention to the problem that when proton leaves a water molecule it should have a charge $q_H = e$. In fact it is possible to introduce an analytical switching function for protons belonging to the cation first coordination sphere with the purpose to have long-range part of two-body potentials for particles of broken water molecules different than for particles confined in CF1 molecules. However this would be more complicated approach which will require several more species of particles to be considered in MD and as the initial step we neglect this problem and will consider effective charges even in the case of decay of water molecules.

For MD we use the ‘shifted-force’ procedure for potentials of interparticle interactions [27–29] to avoid time consuming Ewald-like summation for long-range potentials and their spatial derivatives. We performed for bulk CF1-water two pilot MD runs: one with the ‘shifted-force’ potentials and the second with taking into account long-range Coulombic tails by Ewald summation. In both cases the radial distribution functions were obtained almost identical. Another advantage of using the ‘shifted-force’ potentials was the fact, that effectively one gets the system with two-body potentials like in non-ionic liquids, which vanish on the $r_{cut} = L/2$ with L being the linear scale of MD-box. Hence, one should not care about the neutrality condition and hence, the presence of anion can be dropped, that reduces the number of components of the system.

The two-body potentials of interaction between cation M^{Z+} and water molecules we use a Na^+ -like model [22,23].

$$U_{M^{Z+}O}(r) = \frac{218.790}{r} \cdot Z - \frac{36.677}{r^2} + 116862 e^{-4.526r}$$

$$U_{M^{Z+}H}(r) = \frac{109.395}{r} \cdot Z + \frac{7.479}{r^2} + 99545 e^{-7.06r} \quad (3)$$

where Z is the cation valency.

3. Results and discussion

3.1. Simulation details and conditions

The standard molecular dynamics simulations within microcanonical ensemble for the system of 342 water molecules and one positively charged ion were performed over $8.5 \cdot 10^5$ time steps for each value of the charge (+1, ..., +6). The equations of motion were integrated by predictor-corrector Gear algorithm of fourth order with the time step $\tau = 10^{-16} s$. The density and averaged temperature of the system were 1000 kg/m^3 and 298K, respectively. We would like to add here a note about temperature control during MD in this study. For the case of highly ionized cation, when the process of decay of a water molecule occurred, the excess of kinetic energy led to increasing the temperature. After we found the change in averaged temperature due to decay of water molecule the equilibration over $2 \cdot 10^4$ timesteps was performed and the production run was restarted.

3.2. Radial pair distribution functions

The formation of hydrogen shell around cation M^{Z+} and hydrolysis effects are characterized by the radial distribution functions ion-oxygen $g_{MO}(r)$ and ion-hydrogen $g_{MH}(r)$ and the corresponding running integration numbers:

$$n_{M\alpha}(r) = 4\pi\rho_{\alpha} \int_0^r g_{M\alpha}(r') r'^2 dr' \quad (4)$$

where ρ_{α} is the number density of the atoms of kind α .

The Fig. 1 shows $g_{MO}(r)$ and $n_{MO}(r)$ functions for three different cations valencies. One can find that for higher cation charges the general tendency is the shift of first and second peaks of $g_{MO}(r)$ and displacement to smaller distances. These effects are connected with the increasing of electrostatic attraction between cation and oxygens. Also, the amplitude of the first peak gets higher. Already, for $Z = +2$ there opens a gap between the first and second peaks. This gap can be seen on the running coordination number $n_{MO}(r)$ in Figure 1b as a plateau in the region

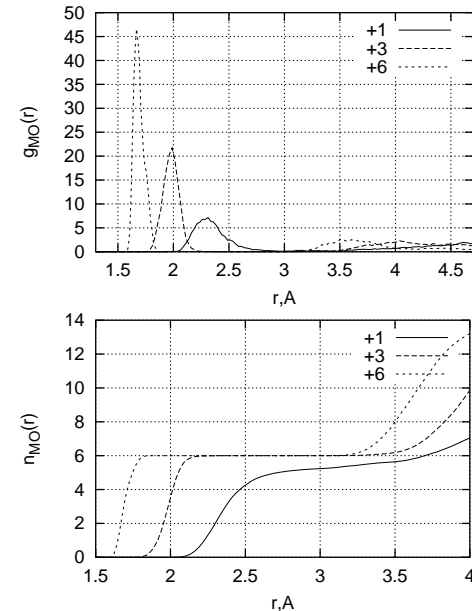


Figure 1. Radial distribution function cation-oxygen $g_{MO}(r)$ (a) and relevant running coordination number $n_{MO}(r)$ for cation charges $Z = +1$ (solid line), $Z = +3$ (dashed line) and $Z = +6$ (dash-dotted line).

$\sim 2 - 3 \text{ \AA}$. By increasing the cation charge starting from $Z = +2$ one gets always six nearest oxygens octahedrally arranged around cation in the sphere of $\sim 3 \text{ \AA}$. Since the first peak of $g_{MO}(r)$ gets shifted towards smaller distances, this means that higher cation charges make nearest six oxygen atoms more bounded due to electrostatic forces. Such a formation of the cation, six oxygens and relevant hydrogens can be considered as a cluster MO_6H_x .

The situation with hydrogens in the region close to the cation is more complicated. One can see in Figure 2a, that the second maximum of the radial distribution function cation-hydrogen $g_{MH}(r)$ is shifted towards smaller distances as it was with the cation-oxygen RDF. However, the first maximum of $g_{MH}(r)$ is shifted to the distance $\sim 2.75 \text{ \AA}$ only by increasing the cation charge to the value $Z = +3$. By further increasing the charge Z the first peak does not exhibit shift to smaller distances, but the amplitude of the first peak gets smaller. The situation becomes more clear by considering the running coordination number $n_{MH}(r)$ in

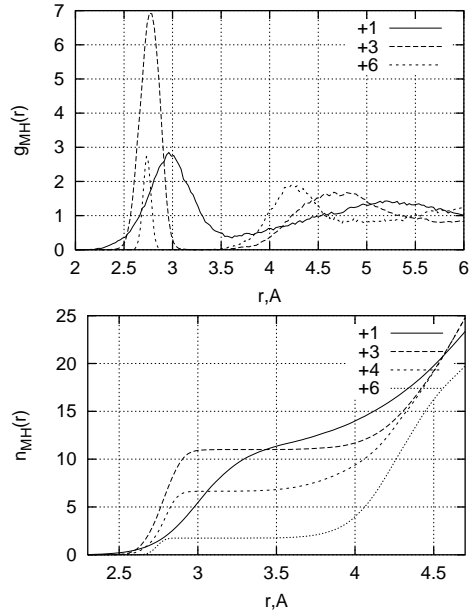


Figure 2. Radial distribution function cation-hydrogen $g_{MH}(r)$ (a) and relevant running coordination number $n_{MH}(r)$ for cation charges $Z = +1$ (solid line), $Z = +3$ (dashed line) and $Z = +6$ (dash-dotted line).

Figure 2b. For $Z = +3$ there appears a plateau with 12 hydrogens, which belong to six stretched water molecules. The oxygens of these six water molecules are oriented towards cation. By increasing the cation charge the stretched water molecules begin to decay. For $Z = +4$ there remain only seven hydrogens in the cation shell. And, for very large value of cation charge all molecules have lost one or two hydrogens. Thus, for $Z = +6$ we obtain a formation, which consists of one cation, six oxygens and two hydrogens MO_6H_2 .

The influence of cation valency on the hydration shell is visually demonstrated on Figure 3 and is also summarized in table 1. There is also presented a number of protons lost by hydration shell:

$$\hat{h} = 2n_{MO}(r_{min}) - n_{MH}(r_{min}). \quad (5)$$

The radial distribution functions $g_{OO}(r)$, $g_{OH}(r)$, $g_{HH}(r)$ characterize the influence of cation on the structure of water. We should note that these functions are averaged over all water molecules, which are in

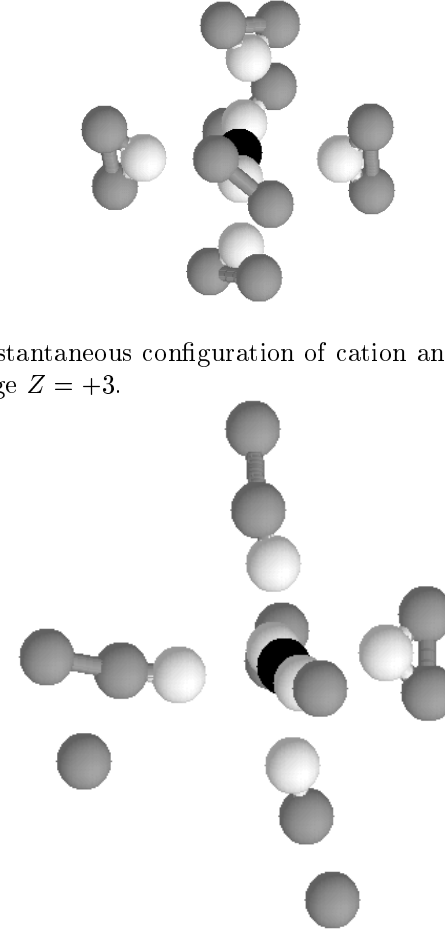
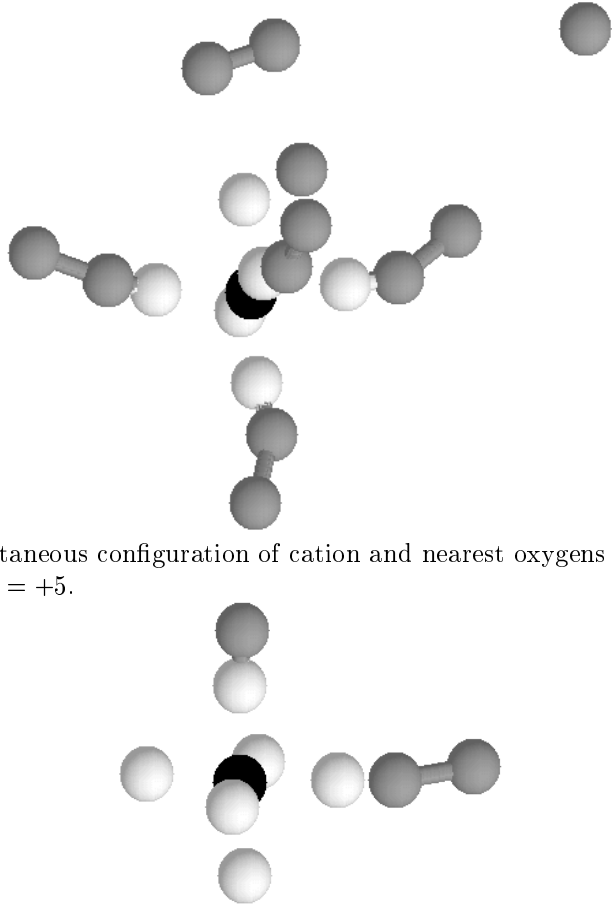


Figure 3. a) Instantaneous configuration of cation and nearest oxygens for cation charge $Z = +3$.

b) Instantaneous configuration of cation and nearest oxygens for cation charge $Z = +4$.



c) Instantaneous configuration of cation and nearest oxygens for cation charge $Z = +5$.

d) Instantaneous configuration of cation and nearest oxygens for cation charge $Z = +6$.

Table 1. Cation valency influence on hydration shell parameters

	$r_{max1}, \text{\AA}$	$g(r_{max1})$	$r_{min1}, \text{\AA}$	$n(r_{min1})$	\hat{h}	$r_{min2}, \text{\AA}$	$n(r_{min2})$
M^+O	2.312	7.145	3.062	5.268	-1.281	5.362	24.545
M^+H	2.962	2.847	3.612	11.817		-	-
$M^{2+}O$	2.112	16.565	2.6-3.1	5.999	-0.022	5.112	20.759
$M^{2+}H$	2.862	5.900	3.412	12.020		5.812	53.185
$M^{3+}O$	1.988	21.700	2.39-3.11	5.999	0.999	4.888	19.943
$M^{3+}H$	2.862	6.930	3.21-3.29	10.999		5.888	54.920
$M^{4+}O$	1.838	24.178	2.21-3.06	5.999	5.357	5.012	22.002
$M^{4+}H$	2.788	5.736	3.088	6.641		5.788	50.496
$M^{5+}O$	1.712	33.416	2.11-3.04	5.999	8.158	4.912	19.422
$M^{5+}H$	2.762	4.177	2.99-3.09	3.840		5.838	47.745
$M^{6+}O$	1.688	46.617	1.88-3.04	5.999	10.248	4.206	14.086
$M^{6+}H$	2.731	2.726	2.87-3.42	1.750		4.744	20.416

cation shell and in bulk far away from the cation, so that only the weak effect of cation onto nearest water molecules can be visible.

In Figures 4a,b,c one can see how these radial distribution functions are changed by the presence of cation with charges $Z = +2$ and $Z = +6$ in comparison with the case of pure CF1 water. For small values of cation charge the effect is rather minimal, while for $Z = +6$ the radial distribution functions get new features:

- i) there appears a well pronounced shoulder on $g_{OO}(r)$ at $r \sim 2.3\text{\AA}$;
- ii) in the gap between intramolecular and intermolecular parts of the function $g_{OH}(r)$ at $r \sim 1.3\text{\AA}$ appears well pronounced maximum;
- iii) the first intermolecular peak of $g_{HH}(r)$ is sufficiently increasing.

The shoulder on $g_{OO}(r)$ is connected with the specific behaviour of $g_{MO}(r)$ (Fig. 1) which shows that for the hexavalent cations the averaged distance between cation and nearest oxygens is $\sim 1.7\text{\AA}$ for $Z = +6$. We can see in Figure 3, where an instantaneous configuration of the cation and nearest six oxygens is presented that all six oxygens are strongly octahedrally arranged around the cation. Thus, taking this fact into account, we obtain the smallest distance between oxygen atoms in a cluster to be of order $1.7 \cdot \sqrt{2}$, that is 2.4\AA . And, this is just the position of a shoulder on $g_{OO}(r)$ for the cation charge $Z = +6$.

Another specific feature of RDFs in the ‘charged cation-flexible water’ model was observed on $g_{OH}(r)$ as a small maximum at $\sim 1.35\text{\AA}$ for high values of Z . The analysis of distances between oxygens and hydrogens leads to a conclusion, that some of free protons are located near the

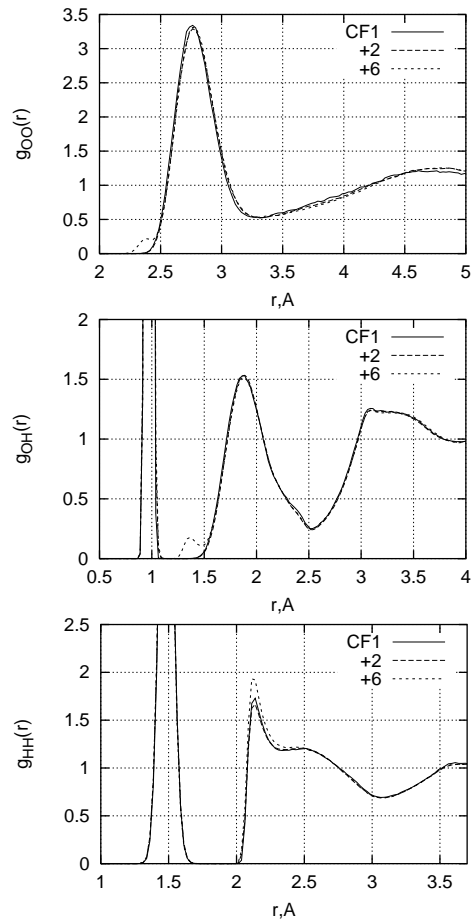


Figure 4. Radial distribution functions $g_{OO}(r)$, $g_{OH}(r)$, $g_{HH}(r)$ for pure CF1 water (solid line) and with cation charges $Z = +2$ (dashed line) and $Z = +6$ (dash-dotted line).

oxygens of water molecules of the second cation shell. Such a formation is shown in Figure 5. In fact, this corresponds to a water molecule with an extra proton, the hydroxonium (H_3O^+).

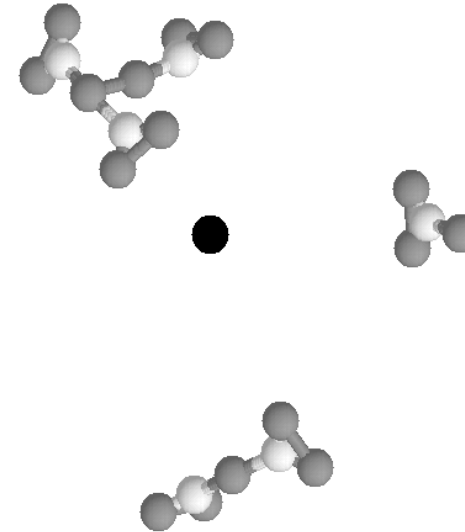


Figure 5. Clusters in the cation shell for cation charge $Z = +6$

The obtained results for configurations H_3O^+ , $H_5O_2^+$ and higher hydrated proton clusters are in qualitative agreement with the corresponding results obtained in the framework of ab initio molecular dynamics simulation [30]. However for quantitative agreement our description needs an improvement connected with change of proton charge after the decay of water molecule.

There also exists the possibility for proton to be trapped between two oxygens of neighbour molecules beyond the first cation shell. Such a case of two water molecules bounded by an extra hydrogen bond is shown in Figure 5 too. In fact, such a formations can be stable and even produce chain of water molecules in the case of many extra protons in the system.

The obtained radial distribution functions can be used for calculation of hydration energy of cation [22]

$$E_{M^{z+}}^{hydr} = 4\pi \sum_{\alpha=O,H} \rho_{\alpha} \int_0^{\infty} r^2 g_{M\alpha}(r) U_{M\alpha}(r) dr \quad (6)$$

The obtained results are presented on Figure 6

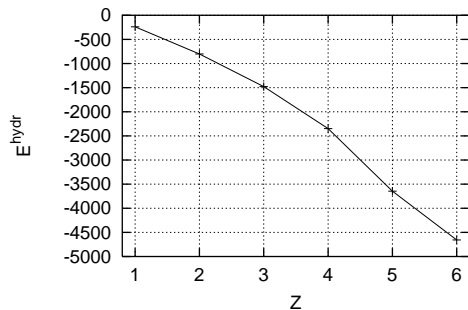


Figure 6. Hydration energy E^{hydr} of cation in dependence of its valence Z .

3.3. Velocity autocorrelation functions

As usually for the description of dynamical properties we consider the velocity autocorrelated functions (VACF). The normalized VACF of cation with different valency

$$\psi_{M^{z+}}(t) = \frac{\langle v_M(0)v_M(t) \rangle}{\langle (v_M(0))^2 \rangle} \quad (7)$$

are shown on Figure 7. $v_M(t)$ is the velocity of cation at time t .

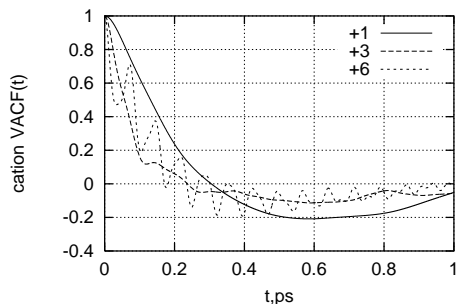


Figure 7. Cation velocity autocorrelation functions for cation charges $Z = +1$ (shown by solid line), $Z = +3$ (dashed line) and $Z = +6$ (dash-dotted line).

For monovalent cation ($Z = 1$) $\psi_M(t)$ has a regular form inherent to atoms of simple liquids. A wide minimum at $t \approx 0.6ps$ is the consequence

of cage effect, when the cation changes its velocity backwards due to scattering on water molecules. By increasing the value of cation charge the shape of VACFs gets affected by weakly pronounced oscillations at $Z = +3$, which become rather strong when the cation charge increases to $Z = +6$. Well pronounced oscillations on VACF have approximately a period of $0.06ps$. Usually such a kind of oscillations implies existence of normal modes in some bounded group of atoms. Thus, the cation VACFs are in agreement with analysis of RDFs when we supposed, that for cation charge $Z = +6$ a cluster MO_6H_x can be formed.

The spectral density of the hindered translation motion has been calculated by Fourier transformation of $\psi_M(t)$:

$$\tilde{\psi}_{M^{z+}}(\omega) = \int_0^{\infty} \frac{\langle v_M(0)v_M(t) \rangle}{\langle (v_M(0))^2 \rangle} \cos(\omega t) dt \quad (8)$$

The result is presented on Figure 8

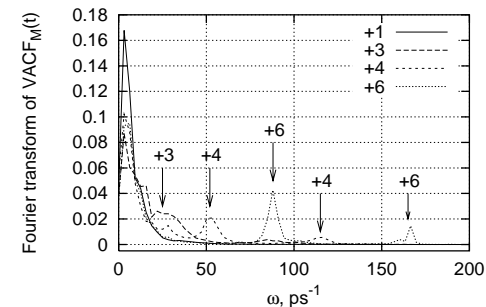


Figure 8. Fourier transforms of cation velocity autocorrelation functions for cation charges $Z = +1$ (shown by solid line), $Z = +3$ (dashed line), $Z = +4$ (short-dashed line) and $Z = +6$ (dotted line).

One can see the following features on the Fourier transforms of cation VACFs $\tilde{\psi}_{M^{z+}}(\omega)$:

- i) the low-frequency region of $\tilde{\psi}_{M^{z+}}(\omega)$ ($\omega \sim 0 - 20ps^{-1}$) corresponds to the regular picture of diffusive motion of particles. By increasing valency Z the amplitude of main peak of $\tilde{\psi}_{M^{z+}}(\omega)$ gets smaller. Also, the value $\tilde{\psi}_{M^{z+}}(0)$ decreases, that means the reduction of diffusion coefficient. This can be easily understood by accepting, that higher cation charges make more rigid shell around cation, which can move much slower than bare cation;
- ii) for $Z = +2$ there appears a shoulder at $\omega \sim 25ps^{-1}$, which gets

shifted to the region of higher frequencies and for $Z > +3$ instead of the shoulder one observes already separated group of frequencies. For the sequence $Z = +4, +5, +6$ this separated peak gets shifted to the region of higher frequencies ($\omega \sim 50 - 90 ps^{-1}$) and gets more narrow; iii) for the sequence $Z = +4, +5, +6$ one observes the emergence of additional groups of very high frequencies ($\omega \sim 120 - 180 ps^{-1}$). For $Z = +6$ such a maximum gets very narrow ($\omega \sim 155 - 175 ps^{-1}$).

The separated groups of frequencies, visible on spectral representation of cation VACFs, correspond to normal modes, which emerge when the hydration shell gets more rigid by increasing the cation charge.

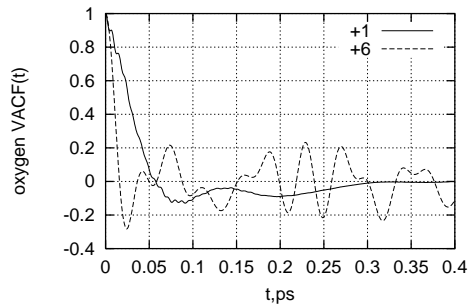


Figure 9. Velocity autocorrelation functions for oxygens, which were found at $t = 0$ in vicinity of cation. Solid, dashed and dash-dotted lines correspond to cation charges $Z = +1, +3, +6$, respectively.

The normalized velocity autocorrelation functions

$$\psi_O(t) = \frac{\langle v_O(0)v_O(t) \rangle}{\langle (v_O(0))^2 \rangle} \quad (9)$$

of oxygens, which at $t = 0$ were found inside the sphere with $R = 5\text{\AA}$ around the cation, are shown in Figure 9 for the different cation charges ($Z=+1,+3,+6$). For the smallest value of cation charge $Z = +1$ the function $\psi_O(t)$ is very close to the regular VACF of oxygen for CF1 model. This implies, that the smallest cation charge does not affect sufficiently the diffusion of water molecules. The VACF for $Z = +1$ shows weak modulation by short-period intramolecular oscillations in CF1 water molecules. By increasing the cation charge the effect of intramolecular oscillations gets negligible, but as it was in the case of cation VACFs the functions get modulated by normal modes of a rigid cation shell, which involve cations and oxygen atoms.

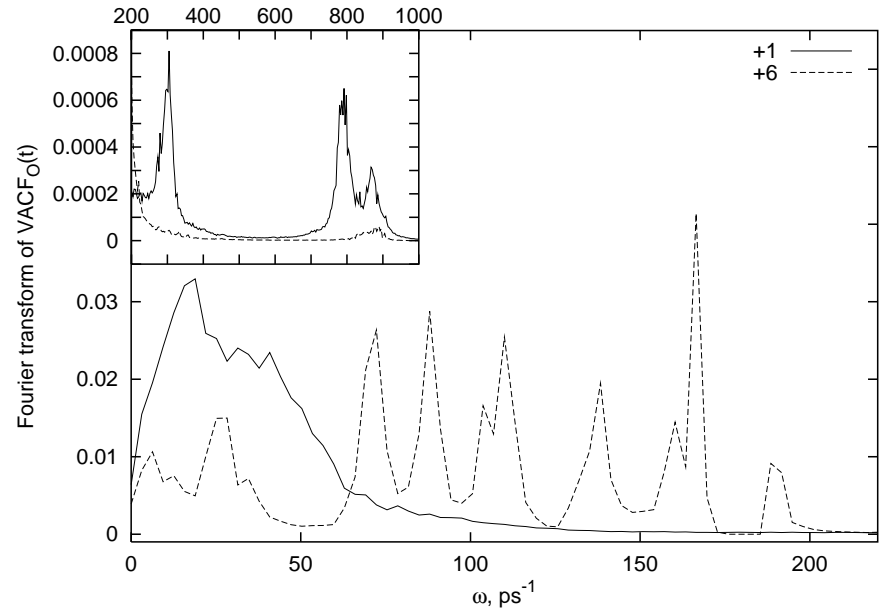


Figure 10. Fourier transforms of oxygen velocity autocorrelation functions for cation charges $Z = +1$ (shown by solid line), $Z = +3$ (dashed line) and $Z = +6$ (dash-dotted line).

The spectral analysis of oxygen VACFs allows to see the following features in Figure 10:

- i) for $Z = +1$ one observes contributions of very high-frequency intramolecular oscillations onto motion of oxygen ions connected with the specific orientational structure of water formed the H-bond network. With increasing of cation charge we have the local destruction of the tetrahedral arrangement of water molecules. For high cation charges ($Z > +3$) the effect of very high-frequency group of oscillations almost disappears due to strong stretching of water molecules in hydration shell and losing hydrogens;
- ii) it is clearly seen, that by increasing the cation charge from $Z = +1$ to $Z = +6$ the regular diffusive motion of oxygen ions close to cation is transformed into some normal oscillations of strongly bounded cation shell, which consists of cation, six nearest oxygens and several hydrogens.

The comparison of the spectral density of the hindered translation motion of cation and oxygens in hydration shell (Fig. 8 and Fig. 10)

shows that two characteristic frequencies for highly charged cations coincide exactly with characteristic frequencies of oxygens in hydration shell. Thus, the obtained velocity autocorrelation functions strongly support our results obtained from the analysis of the radial distribution functions about the stability of the cluster of six oxygens with octahedral configuration around the highly charged cation. At the same time in the spectra of oxygen in the presence of cation the four new characteristic frequencies appear. They are connected with libration motions of oxygens in octahedral complexes. The obtained results are confirmed by the recent investigations [31] of the Raman spectra of aqueous solutions of aluminium chloride. Due to this work there exists a coupling between vibrational oscillations of the hydrate with librational motions of the water molecules coordinated by the aluminium cation.

4. Conclusions

- i) A simple model of flexible CF1 water molecules with 'shifted-force' two-body potentials is used for a molecular dynamics study of a qualitative picture of hydrolysis due to highly charged cations in liquid;
- ii) Our results show, that within the proposed model we obtain hydrolysis effect when the cation charge is large enough. Water molecules near the cation start decaying at $Z = +4$, while for smaller cation charges the water molecules are sufficiently stretched;
- iii) For highly charged cations our model leads to formation of clusters MO_6H_x with number of hydrogens $x = 12; 7; 4; 2$ for the sequence of cation charges $Z = +3; +4; +5; +6$. For our model there exist always six oxygens in these clusters;
- iv) The six oxygens around the highly charged cation form a cluster with octahedral configuration;
- v) It is shown, that the hydrogens, which left the water molecules, can form hydroxonium and additional hydrogen bonds between water molecules;
- vi) Our analysis of velocity autocorrelation functions supports the picture of cluster formation around the cation. It is shown, that by increasing the cation charge there appear separated groups of frequencies in spectral representation of velocity autocorrelation functions. These separated groups of frequencies correspond to normal modes in the cluster formation.

5. Acknowledgement

This study was performed in frames of the project INTAS-Ukraine-95-0133. We are grateful to I.R.Yukhnovskii for permanent interest to our results and P.Bopp for fruitful discussion. We also like to thank to A.M.Gaspar for the possibility to familiarize ourselves with her results in detail [31].

References

1. C.F.Baes, R.E. Mesmer. *The Hydrolysis of Cations* (Wiley: New York), 1976
2. J.Livage, M.Henry, C.Sanchez. *Progr. Solid State Chem.* **18**, 259, 1988
3. M.F.Holovko, *Cond. Matt. Phys.* **12**, 57, 1997
4. W.Stumm, J.J.Morgan, *Aquatic Chemistry*, (Wiley: New York), Interscience, 1981
5. C.M.Chang, M.K.Wang. *Chem.Phys.Lett.*, **286**, 46, 1998
6. K.Heinzinger, P.C.Vogel, *Z. Naturforsch.* **29a**, 1164, 1974
7. F.H.Stillinger, A.Rahman, *J.Chem.Phys.* **60**, 1545, 1974
8. K.Heinzinger in *Ions and Molecules in Solution. Studies in Physical and Theoretical Chemistry* edited by N.Tanaka, H.Ohtaki, R.Tamamushi (Elsevier, Amsterdam) **27**, 61, 1983
9. K. Heinzinger. in *Computer Modeling of Fluids, Polymers and Solids* edited by C.R.A.Catlow, S.C.Parker, M.Allen (Dordrecht, Kluwer Academic Publ.) 357, 1990
10. H.L.Lemberg, F.H.Stillinger, *J.Chem.Phys.* **62**, 1677, 1975
11. F.H.Stillinger, A.Rahman, *J.Chem.Phys.* **68**, 666, 1978
12. P.Bopp, G.Jansco, K.Heinzinger, *J.Chem.Phys.Lett.* **98**, 129, 1983
13. M.M.Probst, E.Spohr, K.Heinzinger, P.Bopp. *Molecular Simulation*, **7**, 43, 1991
14. E.Wasserman, J.R.Rustad, S.Xantheas. *J.Chem.Phys.* **106**, 9796, 1997
15. A.Bakker, K.Heinzinger, J.Lindgren, M.M.Probst, P.P.Bopp, *Int. J. Quant. Chem.* **75**, 659, 1999
16. D.Marx, M.Sprik, M.Parrinello, *Chem. Phys. Lett.* **273**, 360, 1997
17. K.Heinzinger, H.Schafer, *Cond. Matt. Phys.* **2**(18), 273, 1999
18. J.R.Rustad, B.P.Hay, J.W.Halley, *J. Chem. Phys.* **102**, 427, 1998
19. R.L.Martin, P.J.Hay, L.R.Pratt. *J. Phys. Chem.* **A102**, 3565, 1998
20. Yu.P.Davydov, *State of Radionuclides in Solutions*, (Minsk, Nauka, Technika), 1978 (in Russian)

21. R.Bertell. Gulf War Veterans and Depleted Uranium, Haque Peace Conference, 1999
22. M.F.Holovko, Yu.V.Kalyuzhnyi, M.Yu.Druchok, J. Phys. Studies **4**, 100, 2000
23. G.Jansco, K.Heinzinger, P.Bopp, Z. Naturforsch **A40**, 1235, 1985
24. A.Nyberg, A.D.J.Haymet, *Structure and Reactivity in Aqueous Solutions*, edited by D.Trular, C.Kramer (New York, American Chem. Soc.), 1994
25. D.M.Duh, D.N. Perera and A.D.J.Haymet, J.Chem.Phys.**102**, 3736 (1995)
26. P.Bopp (private communication)
27. J.M.Haile, *Molecular Dynamics Simulation: Elementary Methods* (New-York: Wiley), 1992
28. A.D.Trokhymchuk, K.Heinzinger, E.Spohr, M.F. Holovko Mol. Phys. **77**, 903 (1992)
29. J.W.Arthur and A.D.J.Haymet, J.Chem.Phys. **109**, 7991 (1998)
30. D.Weil, D.R.Salahub, J.Chem.Phys. **106**, 6086, 1997
31. A.M.Gaspar, A.J.Kolesnikov, J.C.Li, J.Tomkinson, M. Alves Marques. Abstract of Annual Conference on the Physical Chemistry of Liquids: Molecules-Macromolecules-Biomolecules, Regensburg, Germany, September 08-13, p.21, 2000

Препринти Інституту фізики конденсованих систем НАН України розповсюджуються серед наукових та інформаційних установ. Вони також доступні по електронній комп'ютерній мережі на WWW-сервері інституту за адресою <http://www.icmp.lviv.ua/>

The preprints of the Institute for Condensed Matter Physics of the National Academy of Sciences of Ukraine are distributed to scientific and informational institutions. They also are available by computer network from Institute's WWW server (<http://www.icmp.lviv.ua/>)

Тарас Михайлович Брик
Максим Юрійович Дручок
Мирослав Федорович Головка
Юрій Володимирович Калюжний

МОДЕЛЮВАННЯ ВПЛИВУ ВАЛЕНТНОСТІ КАТІОНА НА ЙОГО
ВЛАСТИВОСТІ У ВОДНИХ РОЗЧИНАХ МЕТОДОМ МОЛЕКУЛЯРНОЇ
ДИНАМІКИ

Роботу отримано 2 квітня 2001 р.

Затверджено до друку Вченою радою ІФКС НАН України

Рекомендовано до друку семінаром відділу теорії рідин

Виготовлено при ІФКС НАН України

© Усі права застережені